Supplementary Information

Decomposition of Methanol-d$_4$ on Rh nanoclusters supported by thin film Al$_2$O$_3$/NiAl(100) under near-ambient-pressure conditions

Guan-Jr Liao[a], Wen-Hao Hsueh[b], Yu-Hsiang Yen[a], Yi-Chan Shih[a], Chia-Hsin Wang[c], Jeng-Han Wang[b],* and Meng-Fan Luo[a],*

[a]Department of Physics, National Central University, No. 300 Jhongda Road, Jhongli 32054, Taiwan

[b]Department of Chemistry, National Taiwan Normal University, No. 88, Sec. 4, Ting-Zhou Road, Taipei, Taiwan

[c]National Synchrotron Radiation Research Center, 101 Hsin-Ann Road, Hsinchu Science Park, Hsinchu 30076, Taiwan

Corresponding authors' Emails:

mfl28@phy.ncu.edu.tw (M.F. Luo); jenghan@ntnu.edu.tw (J.H. Wang)

Figures S1a-c exemplify the STM images for 0.13-, 0.25- and 4.0-ML Rh clusters grown on a thin film of Al_2O_3/NiAl(100) at 300 K. Their size distributions (diameters and heights) are shown in the histograms (insets of the figures). By using the measured mean diameter, height and cluster density for each coverage, we may estimate the surface area of clusters, as a measure of the numbers of Rh surface sites, for each Rh coverage. Table S1 lists the Rh surface areas derived by assuming a half-ellipsoid shape for the cluster.

Figure S2 shows Rh 3d NAP-PES spectra from Al_2O_3/NiAl(100) exposed to CD_3OD at increased pressure from 5×10^{-3} to 0.5 mbar, as indicated, at sample temperature 400 K. Except the negative shift of Rh 3d line induced by increased CD_3OD pressure, the line shape altered little with the pressure, suggesting little altered cluster structures.

Figure S3 shows the density of states (DOS) of surface Rh d band in the four models **Rh$_C$**, **Rh(100)**, **Rh$_{C-OH}$** and **Rh(100)$_{OH}$**. The comparison reveals that **Rh$_C$** has the highest d-band center (-1.95 eV), implying a stronger interaction with adsorbates. The result also shows that the **Rh$_C$** model, the **Rh$_{38}$** cluster, has a great electronic density across the Fermi level, indicating a metallic character.

Figure S4 shows the charge distribution for CH_3OH* on **Rh(100)** and **Rh(100)$_{OH}$**. The formation of hydrogen bond, circled in the plot, enhances the adsorption and

reduces the activation energy for the O-H scission of CH_3OH^*, the initial and also rate-determining step in the methanol decomposition. The promotion in E_{ads} by the hydrogen bonds is also observed in other intermediates, including CH_3O^*, CH_2O^*, CHO^*, in the methanol decomposition. Figure S5a compares E_{ads} of CH_3O^*, CH_2O^* and CHO^* on **Rh$_C$**, **Rh(100)** (without hydrogen bonds), **Rh$_{C-OH}$** and **Rh(100)$_{OH}$** (with hydrogen bonds). Figure S5b illustrates the corresponding adsorption configurations (with hydrogen bonds) on **Rh$_{C-OH}$** and **Rh(100)$_{OH}$**.

Figure S6 compares E_a for the C-H cleavages of $CH_3O^* \rightarrow CH_2O^* \rightarrow CHO^* \rightarrow CO^*$ on **Rh$_C$**, **Rh(100)** (without hydrogen bond), **Rh$_{C-OH}$** and **Rh(100)$_{OH}$** (with hydrogen bond). The hydrogen bond also alters the subsequent dehydrogenation; it could increase or decrease the activation energies. Nevertheless, the alteration is only modest; it is not as great as that for the O-H scission of CH_3OH^* on **Rh$_{C-OH}$**.

Figure S1
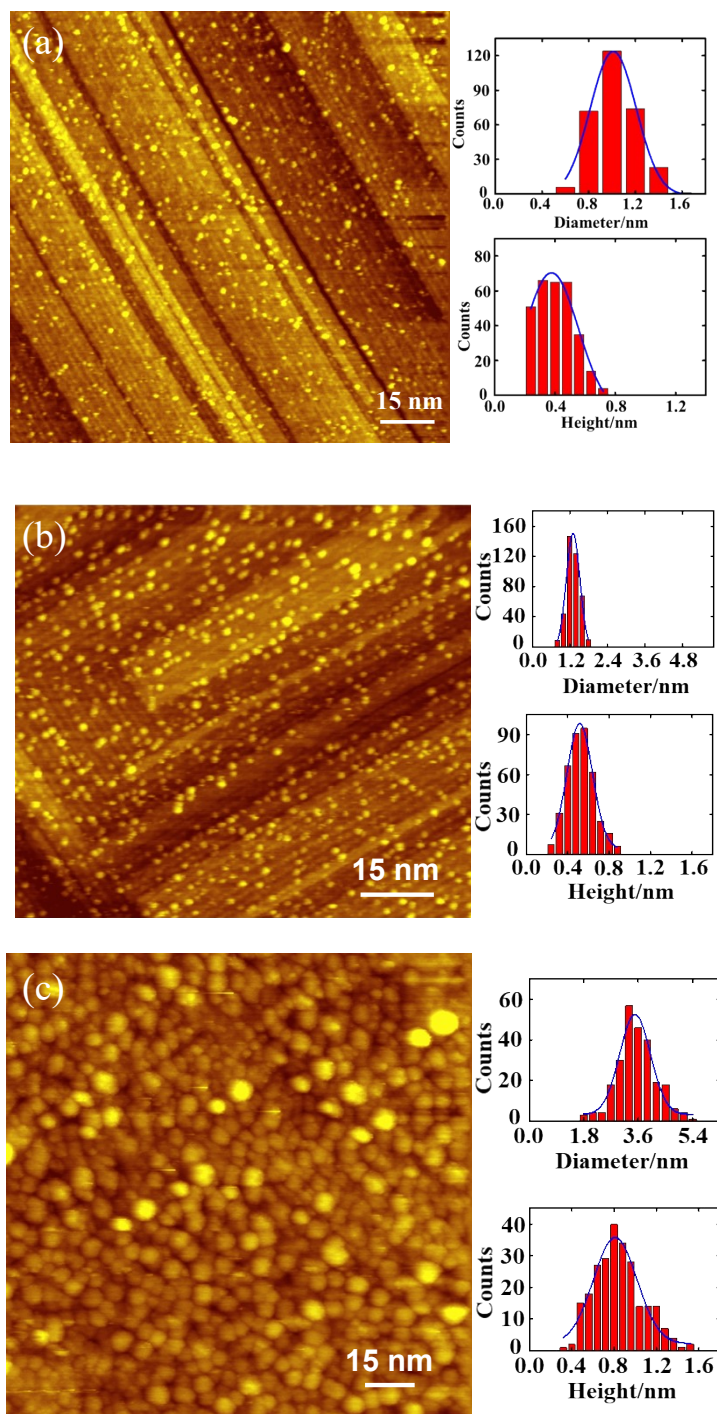
Figure S1. STM image for (a) 0.13-, (b) 0.25- and (c) 4.0-ML Rh deposited on a thin

film of Al_2O_3/NiAl(100) at 300 K. The insets show characteristic histograms of height

and diameter of the clusters; the curves are the best Gaussian fits to the distributions.

Table S1

Coverage (ML)	Mean Height (nm)	Mean Diameter (nm)	Surface Area (nm^2) /per cluster	Surface Area (cm^2) /cm^2
0.13	0.41	1.1	3.18	0.31
0.25	0.52	1.3	4.64	0.48
1	0.78	1.8	9.32	1.49
4	0.8	3.6	25.71	4.16

Table S1. The Rh surface area per cm^2 for each Rh coverage and that for a single cluster at its mean size for each Rh coverage investigated. The surface area for a single cluster was derived by assuming a half-ellipsoid shape for a cluster. The total surface area per cm^2 for each coverage was obtained by the surface area of a single cluster multiplied by the cluster density per cm^2.

Figure S2
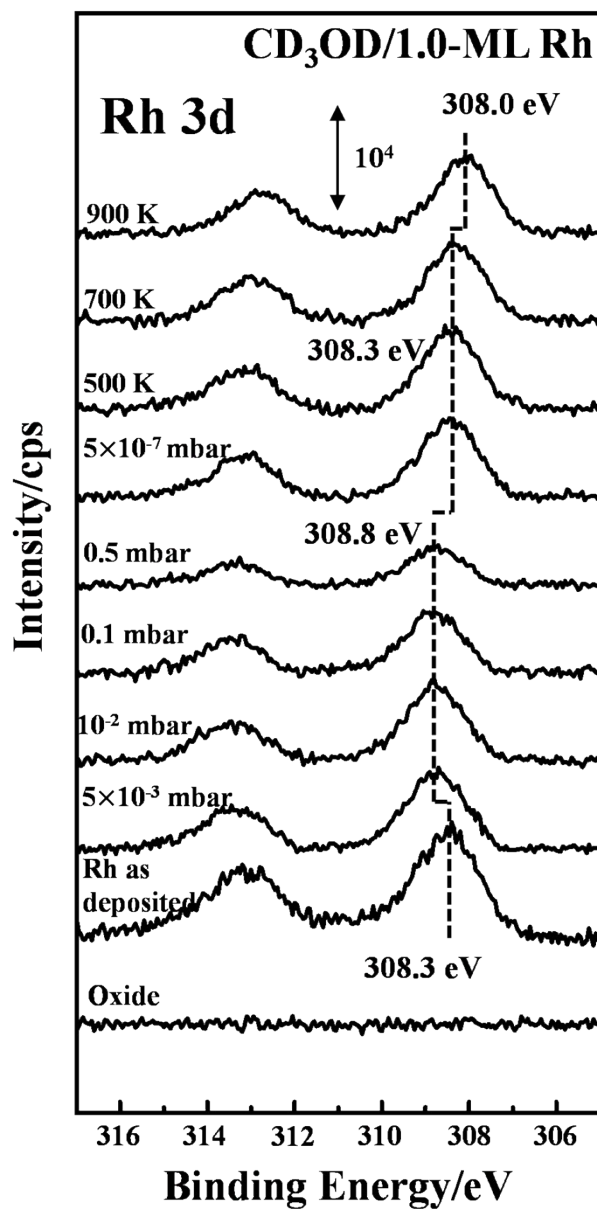
Figure S2. Rh 3d NAP-PES spectra from $Al_2O_3/NiAl(100)$ exposed to CD_3OD at

increased pressure from 5×10^{-3} to 0.5 mbar, as indicated. The Rh clusters were grown

at 300 K and the sample temperature was maintained at 400 K for exposure to CD_3OD.

Figure S3
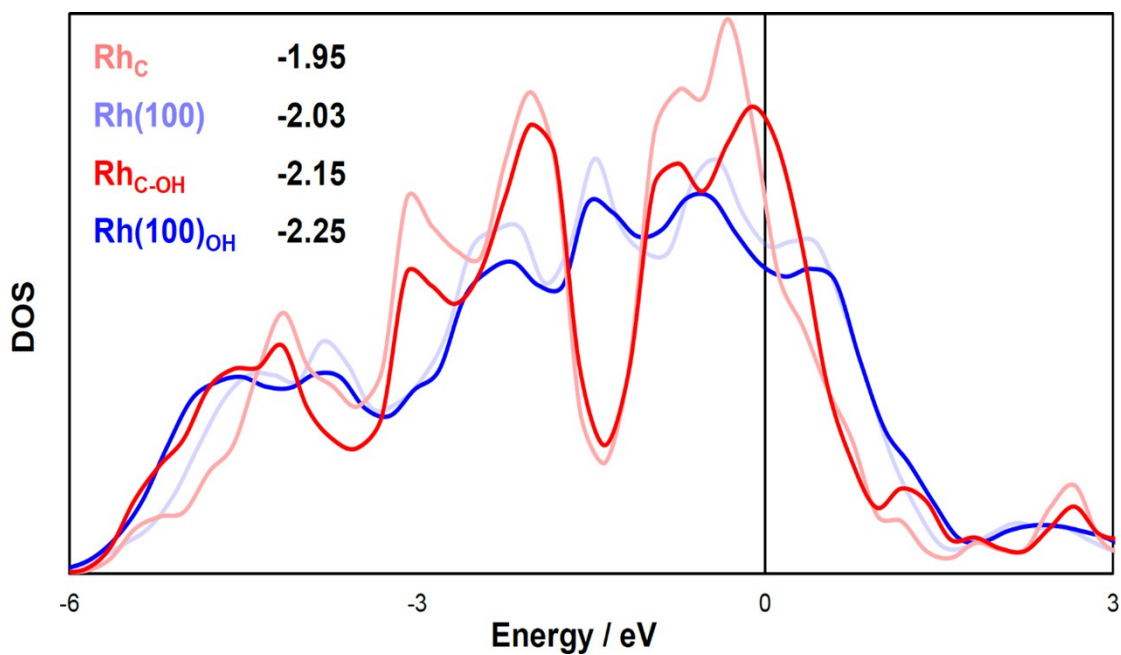
Figure S3. Density of states (DOS) of surface Rh d band in **Rh$_C$**, **Rh(100)**, **Rh$_{C-OH}$** and **Rh(100)$_{OH}$**. The energy 0 indicates the Fermi level and the related d-band centers, in eV, are numbered in the plot. The d-band centers were determined by the following equation:

$$\frac{\int_{-\infty}^{E_F} E\rho_d(E)dE}{\int_{-\infty}^{E_F} \rho_d(E)dE},$$

for which E is the energy, E_F is the Fermi energy and $\rho_d(E)$ is the projected d band density of state (DOS) of the transition metal.

Figure S4
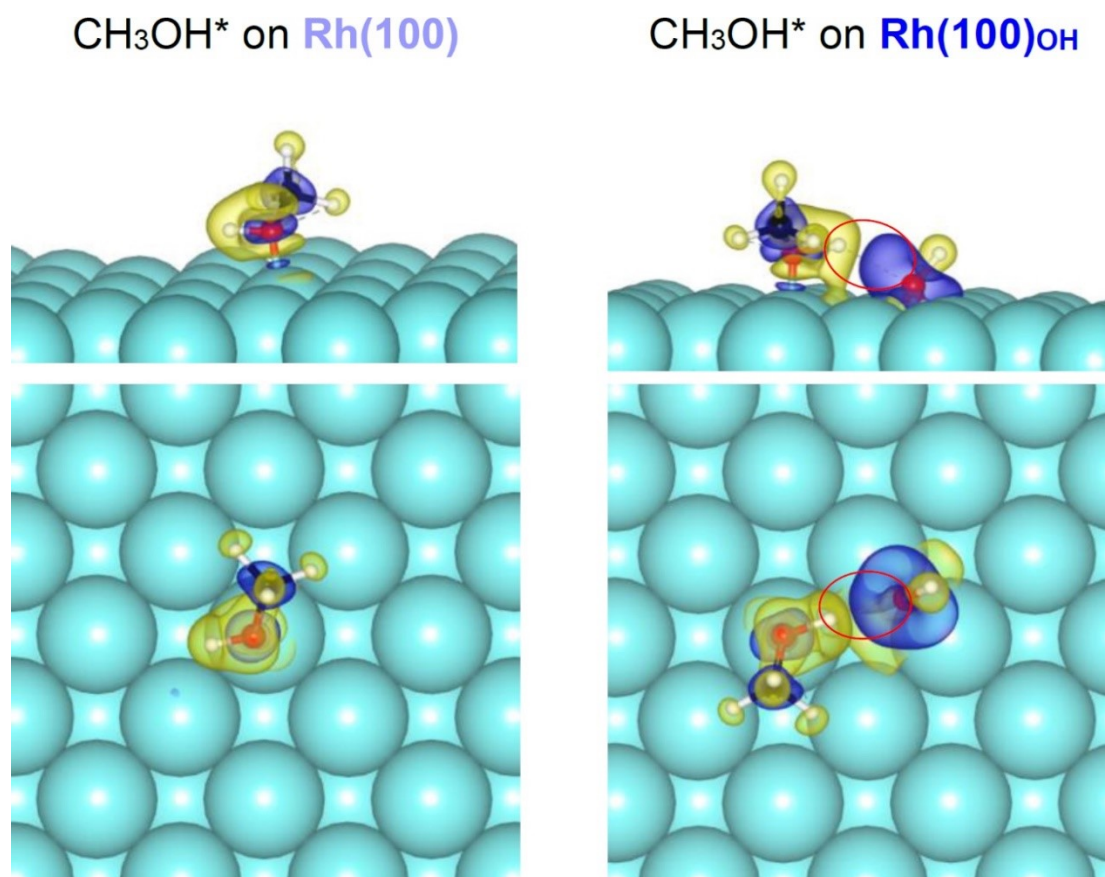
Figure S4. Charge plots for CH$_3$OH* on **Rh(100)** and **Rh(100)$_{OH}$**. Hydrogen bond between CH$_3$OH* and surface OH* on **Rh(100)$_{OH}$** is circled; yellow and blue isosurfaces represent positively and negatively induced charges, respectively.

(a)
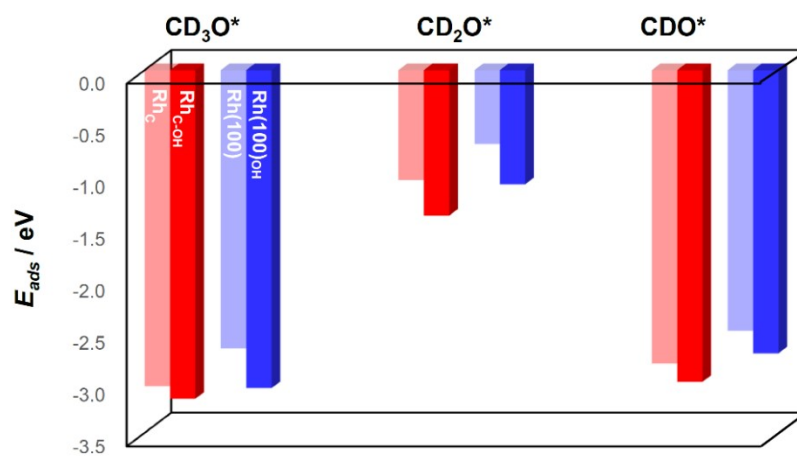
(b)
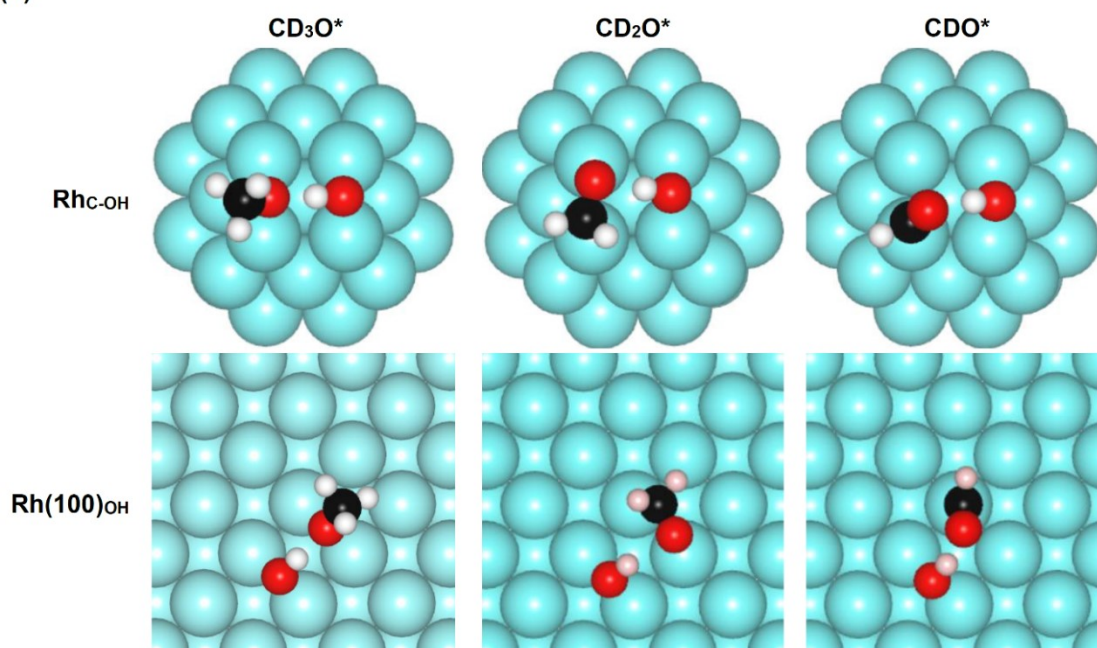
Figure S5. (a) Comparison of E_{ads} of CH$_3$O*, CH$_2$O* and CHO* on **Rh$_C$** and **Rh(100)**

without hydrogen bonds, and on **Rh$_{C\text{-}OH}$** and **Rh(100)$_{OH}$** with hydrogen bonds. (b) The

corresponding adsorption configurations with hydrogen bonds on **Rh$_{C-OH}$** and
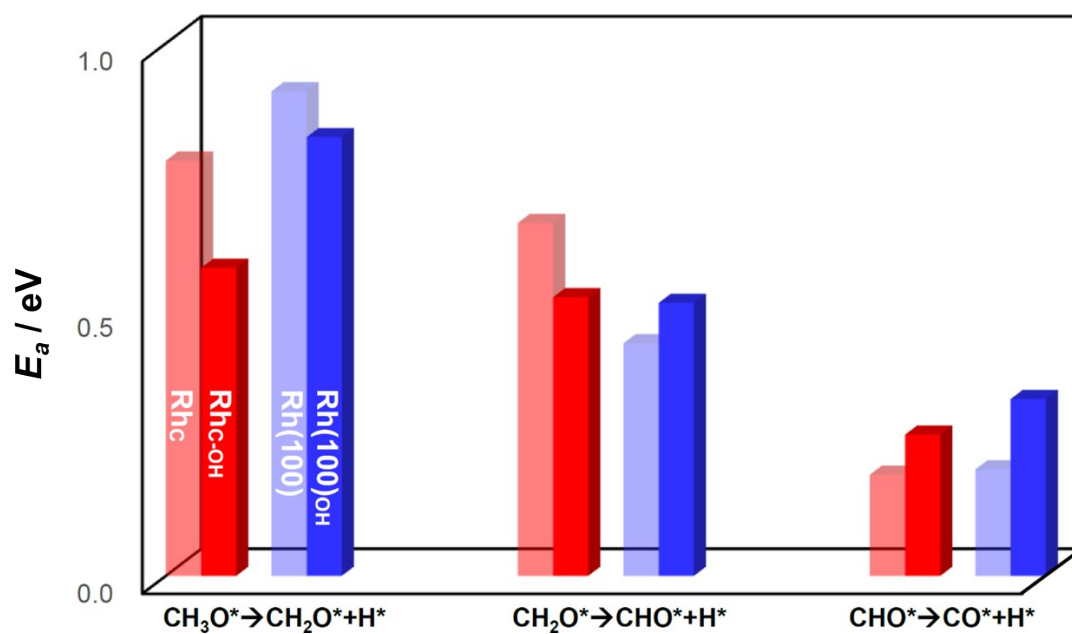
Rh(100)$_{OH}$.

Figure S6

Figure S6. Comparison of E_a for the C-H cleavages of $CH_3O^* \rightarrow CH_2O^* \rightarrow CHO^* \rightarrow CO^*$

on **Rh$_C$** and **Rh(100)** without hydrogen bond, and on **Rh$_{C-OH}$** and **Rh(100)$_{OH}$** with

hydrogen bond.